# Winding up a finite size holographic superconducting ring beyond Kibble-Zurek mechanism

Chuan-Yin Xia[1,2] and Hua-Bi Zeng[2,*]

[1]*Kunming University of Science and Technology, No. 727 South Jingming Road, Cheng Gong District, Kunming, 650500 China*

[2]*Center for Gravitation and Cosmology, College of Physical Science and Technology, Yangzhou University, Yangzhou 225009, China*

(Received 15 September 2020; accepted 29 October 2020; published 1 December 2020; corrected 9 February 2021)

We studied the dynamics of the order parameter and the winding numbers $W$ formation of a quenched normal-to-superconductor state phase transition in a finite size holographic superconducting ring. There is a critical circumference $\tilde{C}$ below which no winding number will be formed; then, $\tilde{C}$ can be treated as the Kibble-Zurek mechanism (KZM) correlation length $\xi$, which is proportional to the fourth root of its quench rate $\tau_Q$, which is also the average size of independent pieces formed after a quench. When the circumference $C \geq 10\xi$, the key KZM scaling between the average value of absolute winding number and the quench rate $\langle |W| \rangle \propto \tau_Q^{-1/8}$ is observed. At smaller sizes, the universal scaling will be modified; there are two regions. The middle size $5\xi < C < 10\xi$ result $\langle |W| \rangle \propto \tau_Q^{-1/5}$ agrees with a finite size experiment observation, while at $\xi < C \leq 5\xi$, the average value of absolute winding number equals the variance of winding number, and there is no exponential relationship between the quench rate and the average value of absolute winding number. The winding number statistics can be derived from a trinomial distribution with $\tilde{N} = C/(f\xi)$ trials, and $f \simeq 5$ is the average number of adjacent pieces that are effectively correlated.

DOI: 10.1103/PhysRevD.102.126005

Phase transition that traverses the critical point at a finite rate is a nonequilibrium process, and the critical dynamics of the out-of-equilibrium process is one of the most interesting and important problems in modern physics [1]. Because of the relaxation time's divergence near the critical point (critical slowing down), the formation of topological defects by taking into account finite speed of propagation of the relevant information was predicted by the Kibble-Zurek mechanism (KZM) [2–9]. The original idea of KZM is from Kibble's insight into the role of causality in structure formation in the early Universe [2,3]. Later, Zurek found that condensed-matter systems offer a test bed to study the dynamics of symmetry breaking [4–6]. He first predicted the formation of independent regions with their average size controlled by the correlation length $\xi$ at the point when the frozen time ends; $\xi$ scales with the linear quench rate $\tau_Q$ in which the phase transition is crossed as a universal power law,

$$\xi \propto \tau_Q^{\alpha}, \tag{1}$$

and the power-law exponent $\alpha = \nu/(1+\nu z)$ is set by a combination of the dynamic and correlation-length (equilibrium) critical exponents denoted by $z$ and $\nu$, respectively. In a spatial $d$-dimensional system, the average density $\tilde{n}$ of the resulting topological defects scales with the linear quench rate as a universal power law,

$$\tilde{n} \propto \tau_Q^{-d\alpha}; \tag{2}$$

this is the key prediction of KZM.

In three-dimensional (3D) and two-dimensional (2D) systems, the topological defects are usually vortex strings [10] and vortices [11,12], respectively, with zeroth order parameter inside the vortex cores. In a one-dimensional (1D) system with real order parameter, kinks are the topological defects with zero order parameter in the center [13]. In a 1D systems with a complex order parameter undergo a phase transition that breaks the $U(1)$ gauge symmetry, winding numbers $W = \oint_C d\theta/2\pi$ are expected to form, but the amplitude of the order parameter keeps uniform [9]. $W$ admits a Gaussian distribution with $\langle W \rangle = 0$; however, the average absolute winding number $\langle |W| \rangle \propto \sqrt{\frac{1}{\xi}} \propto \tau_Q^{-\alpha/2}$ [14,15]. Numerical experiments in a

*Corresponding author.
hbzeng@yzu.edu.cn

quenched superfluid/superconductor have supported Eq. (2) in three dimensions [10], two dimensions [12,16,17], and one dimension [14,15]. In the laboratory, the Eq. (2) has also been confirmed in liquid crystals [18–20], $^3$He superfluids [21,22], Josephson junctions [23–26], thin-film superconductors [27,28], a linear optical quantum simulator [29], and also in a strongly interacting Fermi superfluid [30]. Recently, Adolfo del Campo *et al.* found the universal statistics of topological defects formed in a quantum phase transition beyond KZM [31,32], which has been confirmed by a 1D quantum simulation [33].

Despite the progress, little attention has been devoted to the case when the size of the system approaches the order of $\xi$. Except in experiment [34], the size effect results were reported by L. Corman *et al.* in Bose gases through a temperature quench of the normal-to-superfluid phase transition. Large size $C \gg \xi$ observation matches the KZM prediction by using the mean field theory critical exponents $z = 2, \nu = 1/2$, where $\langle |W| \rangle \propto \tau_Q^{-1/8}$ at fixed $C$ and $\langle |W| \rangle \propto \sqrt{C}$ at a fixed $\tau_Q$ [14,15]. However, at small size $C < 10\xi$, $\langle |W| \rangle \propto \tau_Q^{-0.2}$ at fixed $C$ and $\langle |W| \rangle \propto C^{0.8}$ at a fixed $\tau_Q$ were also reported in Ref. [34]. Now, a theoretical model and even a numerical simulation are still lacking to address the experimental observation. Also, the KZM does not include the case when the system size is not an integer multiple of $\xi$ since at large sizes the remainder can be ignored, and the number of KZM pieces $N$ is always an integer. However, at a finite size close to $\xi$, one has to consider the case of a fractional $N$. Furthermore, equilibrium phase transitions at finite size can still have universal scaling laws, as confirmed in a $^3$He superfluid phase transition [35] and a strongly coupled holographic superconductor [36]; then, it is of importance to study the finite size effect in KZM.

To study the finite size KZM, we adopt a holographic superconductor ring model in the framework of gauge/gravity duality, focusing on the spontaneous formation of winding in the superconducting ring after a temperature quench. The holographic duality [37–39] that relates strongly interacting quantum field theories to theories of classic gravity in higher dimensions has been proven to be a new and useful scheme to study strongly interacting condensed-matter systems in equilibrium [40,41] and also to study the real-time dynamics when the system is far away from equilibrium [42–44]. Then, it is very suitable to study the phase transition dynamics happening at a finite rate [15–17,45–50]. The well-studied holographic superconductor model defined in an anti-de Sitter black hole is [51–53]

$$S = \int d^4x\sqrt{-g}\left[-\frac{1}{4}F^2 - (|D\Psi|^2 - m^2|\Psi|^2)\right]. \quad (3)$$

The metric of the anti-de Sitter black hole in the Eddington coordinates is $ds^2 = \frac{\ell^2}{z^2}(-f(z)dt^2 - 2dtdz + dx^2 + dy^2)$, where $f(z) = 1 - (z/z_h)^3$, and the temperature of the black hole is $T = 3/(4\pi z_h)$. There is a critical value of the black hole temperature below which the charged scalar develops a finite value in the bulk while its dual field theory operator has a finite expectation value $\langle O \rangle$, which breaks the $U(1)$ symmetry in the boundary field theory. Working in 1D spatial boundary geometry by only turning on coordinate $x$ dependence of all the fields in the equations of motion, using the periodic boundary condition in the $x$ coordinate, we are effectively studying a superconducting ring. By solving the dynamic equations by decreasing the black hole temperature cross $T_c$, the quench induced winding number formation process can be monitored in detail [54]. One sample result of a quench from $1.1T_c$ to $0.82T_c$ is given in Fig. 1, where $\tau_Q = e^3$ and $C = 20$. After the quench, the order parameter amplitude approaches the equilibrium value, while the phase develops a stable configuration, the winding number $W = -1$. From the phase configuration in Fig. 1, we can label the position where the phase field increases from $-\pi$ to $+\pi$ to be "+" and the position where the phase field decreases from $+\pi$ to $-\pi$ to be "−" as shown in the last plot, and we find that

$$W = n^+ - n^- = 1 - 2 = -1, \quad (4)$$

where $n^+$ is the number of $+$ and $n^-$ is the number of $-$. We confirmed that the winding number counted from this method always equals exactly the one by integrating $d\theta$ in the closed superconducting ring. Also, the $n^+ + n^-$ is found to be proportional to $C$, which matches the KZM's prediction.

To see how quench rate affects the formation of $W$, people always refer to its variance $\sigma^2(W)$, which is proportional to the number of independent pieces $N = C/\xi \propto \tau_Q^{-1/4}$ using

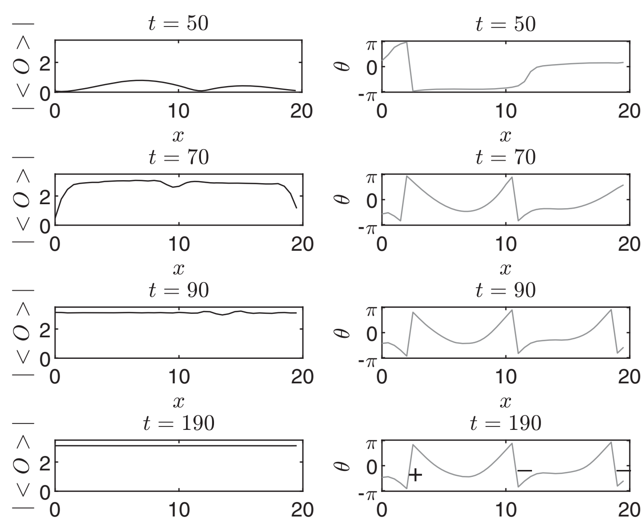


FIG. 1. Winding up a superconducting ring after a temperature quench $\tau_Q = e^3$, the circumference $C = 20$. In the four rows, we show the magnitude of the order parameter $|\langle O \rangle|$ and its phase $\theta$ configuration in the dynamic process. The system finally enters an equilibrium state with constant amplitude of order parameter and a stable configuration of phase field $\theta(x)$.

the mean field exponents $z = 2$ and $\nu = 1/2$ in Eq. (1). At large $N$, $\langle |W| \rangle$ can be computed from the Gaussian distribution, and then we obtain the key prediction at a fixed size [14]

$$\sigma(W) = \sqrt{\langle W \rangle^2} \propto \langle |W| \rangle \propto \tau_Q^{-1/8}, \tag{5}$$

at a fixed rate $\langle |W| \rangle \propto \sigma(W) \propto \sqrt{N}$.

Figure 2 (left) plots $\sigma^2(W)$ as a function of $C$ for different quench rates ($\tau_Q = e^4, e^5, e^6, e^7$), average over 100,000 times calculation. According to KZM, since the system inherits an infinite relaxation time at the critical point, then it cannot catch the speed of a quench, and as a result, the superconducting ring will be divided into many independent pieces with their average size being $\xi(\tau_Q)$. The topological defects forms at the positions where the independent pieces meet, and it is natural to conclude that there will be a critical value of circumference $\tilde{C} = \xi(\tau_Q)$ below which there is only one piece and then no winding number will be formed. The numerical result of $\tilde{C}$ confirmed $\xi(\tau_Q) \propto \tau_Q^{0.244}$ (Fig. 2 inset). Also, from the KZM picture, $\sigma^2(W)[C]$ for different rates can be scaled to exactly one line by transforming $C$ to be the number of pieces formed [Fig. 2 (right)], and in a formula, it can be expressed as

$$\sigma^2(W_{\tau_{Q1}})[C_1] = \sigma^2(W_{\tau_{Q2}})[C_2], \tag{6}$$

when $C_1/\xi(\tau_{Q1}) = C_2/\xi(\tau_{Q2}) = N$. Also, the linear relationship $\sigma^2(W) \propto N$ between the variance of the winding number and number of regions can be seen when the size of regions is roughly larger than 5. Until now, we confirmed the KZM mechanism from another perspective from the size dependent results and the scaling of critical circumference $\tilde{C}$ rather than computing Eq. (2) directly. Note that the agreement also confirmed that a holographic superconducting phase transition is always of the mean field class [55–57].

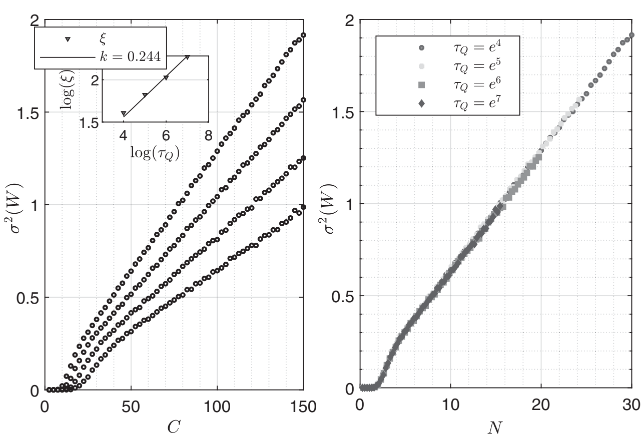


FIG. 2. Size dependence of variance $\sigma^2(W)$. Left: size dependence of $\sigma^2(W)$ for four quench rates, from top to bottom, $\tau_Q = e^4, e^5, e^6, e^7$. The inset shows the scaling of the critical circumference. Right: $\sigma^2(W)$ as a function of pieces number $N$; all quench rate results are identical to each other.

Besides the perfectly matched KZM results, from Fig. 2, one also finds that $\sigma^2(W) \propto N$ cannot hold anymore when the ring size is reducing. Figure 3(b) shows that the non-KZM region is $1 < N \leq 5$. Also in this region, there is another interesting feature that $\sigma^2(W) = \langle |W| \rangle$, since the winding number can have only three values: −1, 0, and 1. One thing that needs to be emphasized is that in this region, though the KZM pieces $N$ can be larger than 1, $W$ does not take a value larger than 1, and this indicates that the formation of topological defects in a size $N \leq 5$ is effectively correlated, which is probably due to the growth of correlation length in the presence of diffusion [13].

Still, in Figs. 3(b) and 3(c), at a larger size $5 < N < 10$, $\sigma^2(W)$ has a linear dependence of $N$, but

$$\langle |W| \rangle \propto N^{0.8}. \tag{7}$$

This is different from the large size result $\langle |W| \rangle \propto N^{0.5}$ [14]. Then, one can conclude that the Gaussian distribution is not good anymore to capture the statistic distribution of winding number at this region. We compared the discrete distribution and the corresponding Gaussian distribution with the variance of $W$ in Fig. 4, which shows the winding distribution at three different numbers of regions $N = 8$, 18, 30. The discrete distribution approaches a Gaussian one when increasing $N$. Since $N < 10$, $|W|$ has only three values from 0 to 2, the deviation from Gaussian distribution is expected. Combining Eq. (7) and

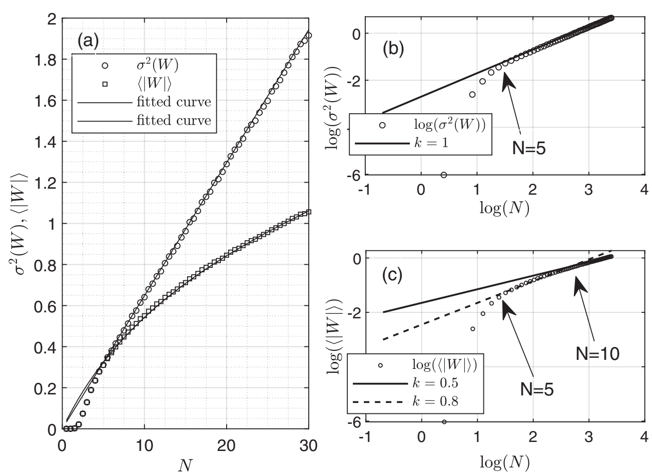


FIG. 3. Size-dependent $\sigma^2(W)$ and $\langle |W| \rangle$. (a) $\sigma^2(W)$ and $\langle |W| \rangle$ as a function of $N$ and their fit from trinomial distribution Eq. (10); when $N < 5$, the two have the same values. (b) Logarithmic relationship between $\sigma^2(W)$ and $N$. (c) Logarithmic relationship between $\langle |W| \rangle$, and $N$. $k$ is the linear fit slop.

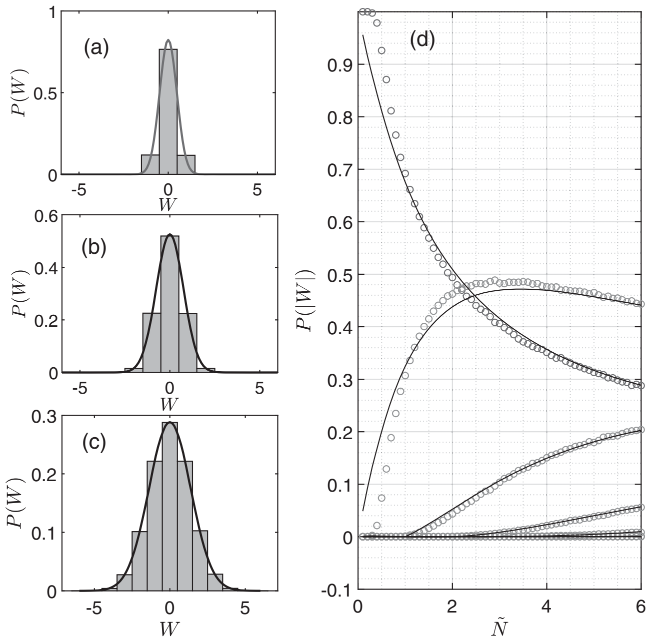


FIG. 4. $P(W)$ and $P(|W|)$. (a–c) Histogram of $P(W)$ for $N = 8$, 18, 30 respectively, when $\tau_Q = e^4$. (d) Numerical results of $P(|W|)$ (circles, from top to bottom are $|W| = 0$, 1, 2, 3, 4, 5, 6, respectively) and their fitted curves derived from Eq. (10) (solid lines).

$$\xi = \frac{C}{N} \propto \tau_Q^{1/4}, \tag{8}$$

we get exactly the beyond KZM scaling between average absolute winding number and quench rate found in experiment [32] when $5 < N < 10$

$$\langle |W| \rangle \propto \tau_Q^{-0.2}. \tag{9}$$

Because the winding number $W = n^+ - n^-$ and we can label the independent pieces to be "+" "−" or "0," it is natural to expect that the distribution of $n^+, n^-$ can be captured by a trinomial distribution. The probability of the trinomial distribution of trials $\tilde{N}$ reads

$$P(\tilde{N}, n^+, n^-) = \frac{\tilde{N}!}{n^0! n^+! n^-!} \left(\frac{p}{2}\right)^{n^+ + n^-} (1 - p)^{n^0}, \tag{10}$$

where $n^0 = \tilde{N} - (n^+ + n^-)$, $n^0$ is the number of pieces without either + or −. $(n^+, n^-, n^0) \le \tilde{N}$, and $\tilde{N}$ equals the largest value of $n^+(n^-)$, which can be defined as the number of effectively unrelated pieces. $p/2$ is the probability for both + and − since the two have the same distribution [58], while $1 - p$ is the 0 probability. From the largest number of $n^+(n^-)$ of a fixed integral $N$, we find that $\tilde{N} = n_{\max}^{+(-)} = N/5$. Furthermore, we consider the case when the $\tilde{N}$ is not an integral; by increasing from $\tilde{N}$ from a smaller integral number $M$ to $M + 1$, the $\sigma^2(W)$ is increasing continuously without a jump. To understand the continuousness of $\sigma^2(W)$, we use the mathematical theorem in which the factorial in Eq. (10) can be expressed by the Gamma function

$$M! = \Gamma(M + 1) = \int_0^\infty y^M e^{-y} dy. \tag{11}$$

With the trinomial distribution, we can calculate the probability $P(|W|)$; for example, $P(W = 0)$ is the summation of the cases where $n^+ = 0 \cup n^- = 0$ and $n^+ = n^-$ in Eq. (10). $P(|W| = 1)$ equals the summation of the cases where $n^+ = n^- \pm 1$. $P(|W|)$ as a function of $\tilde{N} = N/5$ obtained from the trinomial distribution can basically match the numerical results as shown in Fig. 4d, and the best fit parameters were found to be $p = 0.324$. The $P(|W| = 0)$ will keep decreasing when $|W|$ takes larger maximal values due to the increasing numbers of pieces. $P(|W| = 1) = 0$ when $N < 1$, when $N > 1$ $P(|W| = 1)$ keeps increasing to its maximal value at about $\tilde{N} = 2$. $P(|W| = M)$ can only have a finite value when $N > 5M(\tilde{N} > M)$. Another check of the trinomial distribution can be done by computing $\sigma^2(W)$ and $\langle |W| \rangle$ from $P(W)$ obtained from Eq. (10); compare the results to the numerical simulation in Fig. 3. We find good agreement when $N \ge 5(\tilde{N} \ge 1)$. The deviation is obvious when $N < 5(\tilde{N} < 1)$, and in this region with only one effectively independent KZM piece, there are only three possibilities: $n^+ = n^- = 0$; $n^+ = 1, n^- = 0$; and $n^+ = 0, n^- = 1$. Then, $\langle |W| \rangle = \sigma^2(W) = P(n^+ = 1) + P(n^- = 1) = p$, and the probability $p$ is increasing from zero at $N = 1$ to a constant $p = 0.324$ at $N = 5$.

In summary, the numerical experiment in a finite size superconducting ring not only confirms the KZM predictions but also presents new findings of dynamics of phase transition in a superconducting ring. First, the finite size distribution of $W$ is different from Gaussian distribution; then, the KZM scaling law of $\langle |W| \rangle$ will be modified [34]. Second, a continuous version of trinomial distribution with a fractional $\tilde{N}$ trial was proposed to understand the size-dependent statistic distribution of $W$. Furthermore, the numerical results indicate the effective independent pieces $\tilde{N} = L/5\xi$, where $\tilde{N}$ still admits the scaling law predicted by the Kibbe-Zurek mechanism. Finally, the nonlinear dependence between $\sigma^2(W)$ (topological defect number in other condensed-matter systems) and $N$ was found at small size $\tilde{N} \le 1$, which is expected to be a universal property in finite size KZM that can be checked by experiments.

## ACKNOWLEDGMENTS

We thank Hai Qing Zhang and Wei Can Yang for valuable discussions. This work is supported by the National Natural Science Foundation of China (under Grant No. 11675140).

[1] S. Sachdev, *Quantum Phase Transitions*, 2nd ed. (Cambridge University Press, Cambridge, England, 2011).
[2] T. W. B. Kibble, J. Phys. A **9**, 1387 (1976).
[3] T. W. B. Kibble, Phys. Rep. **67**, 183 (1980).
[4] W. H. Zurek, Nature (London) **317**, 505 (1985).
[5] W. H. Zurek, Acta Phys. Pol. B **24**, 1301 (1993).
[6] W. H. Zurek, Phys. Rep. **276**, 177 (1996).
[7] J. Dziarmaga, Adv. Phys. **59**, 1063 (2010).
[8] A. Polkovnikov, K. Sengupta, A. Silva, and M. Vengalattore, Rev. Mod. Phys. **83**, 863 (2011).
[9] A. del Campo and W. H. Zurek, Int. J. Mod. Phys. A **29**, 1430018 (2014).
[10] N. D. Antunes, L. M. A. Bettencourt, and W. H. Zurek, Phys. Rev. Lett. **82**, 2824 (1999).
[11] M. B. Hindmarsh and A. Rajantie, Phys. Rev. Lett. **85**, 4660 (2000).
[12] A. Yates and W. H. Zurek, Phys. Rev. Lett. **80**, 5477 (1998).
[13] P. Laguna and W. Hubert Zurek, Phys. Rev. Lett. **78**, 2519 (1997).
[14] A. Das, J. Sabbatini, and W. H. Zurek, Sci. Rep. **2**, 352 (2012).
[15] J. Sonner, A. del Campo, and W. H. Zurek, Nat. Commun. **6**, 7406 (2015).
[16] P. M. Chesler, A. M. Garcia-Garcia, and H. Liu, Phys. Rev. X **5**, 021015 (2015).
[17] H.-B. Zeng, C.-Y. Xia, W. H. Zurek, and H.-Q. Zhang, arXiv:1912.08332.
[18] I. Chuang, B. Yurke, R. Durrer, and N. Turok, Science **251**, 1336 (1991).
[19] M. J. Bowick, L. Chandar, E. A. Schik, and A. M. Srivastava, Science **263**, 943 (1994).
[20] S. Digal, R. Ray, and A. M. Srivastava, Phys. Rev. Lett. **83**, 5030 (1999).
[21] C. Baeuerle, Y. M. Bunkov, S. N. Fisher, H. Godfrin, and G. R. Pickett, Nature (London) **382**, 332 (1996).
[22] V. M. H. Ruutu, V. B. Eltsov, A. J. Gill, T. W. B. Kibble, M. Krusius, Yu. G. Makhlin, B. Plaçais, G. E. Volovik, and W. Xu, Nature (London) **382**, 334 (1996).
[23] R. Carmi, E. Polturak, and G. Koren, Phys. Rev. Lett. **84**, 4966 (2000).
[24] R. Monaco, J. Mygind, and R. J. Rivers, Phys. Rev. Lett. **89**, 080603 (2002).
[25] R. Monaco, J. Mygind, and R. J. Rivers, Phys. Rev. B **67**, 104506 (2003).
[26] R. Monaco, J. Mygind, M. Aaroe, R. J. Rivers, and V. P. Koshelets, Phys. Rev. Lett. **96**, 180604 (2006).
[27] A. Maniv, E. Polturak, and G. Koren, Phys. Rev. Lett. **91**, 197001 (2003).
[28] D. Golubchik, E. Polturak, and G. Koren, Phys. Rev. Lett. **104**, 247002 (2010).
[29] X.-Y. Xu, Y.-J. Han, K. Sun, J.-S. Xu, J.-S. Tang, C.-F. Li, and G.-C. Guo, Phys. Rev. Lett. **112**, 035701 (2014).
[30] B. Ko, J. W. Park, and Y. Shin, Nat. Phys. **15**, 1227 (2019).
[31] A. del Campo, Phys. Rev. Lett. **121**, 200601 (2018).
[32] F. J. Gmez-Ruiz, J. J. Mayo, and A. del Campo, Phys. Rev. Lett. **124**, 240602 (2020).
[33] J.-M. Cui, F. J. Gomez-Ruiz, Y.-F. Huang, C.-F. Li, G.- C. Guo, and A. del Campo, Commun. Phys. **3**, 44 (2020).
[34] L. Corman, L. Chomaz, T. Bienaime, R. Desbuquois, C. Weitenberg, S. Nascimbene, J. Dalibard, and J. Beugnon, Phys. Rev. Lett. **113**, 135302 (2014).
[35] F. M. Gasparini, M. O. Kimball, K. P. Mooney, and M. Diaz-Avila, Rev. Mod. Phys. **80**, 1009 (2008).
[36] A. M. Garca-Garca, J. E. Santos, and B. Way, Phys. Rev. B **86**, 064526 (2012).
[37] J. M. Maldacena, Adv. Theor. Math. Phys. **2**, 231 (1998).
[38] S. S. Gubser, I. R. Klebanov, and A. M. Polyakov, Phys. Lett. B **428**, 105 (1998).
[39] E. Witten, Adv. Theor. Math. Phys. **2**, 253 (1998).
[40] J. Zaanen, Y. W. Sun, Y. Liu, and K. Schalm, *Holographic Duality in Condensed Matter Physics* (Cambridge University Press, Cambridge, England, 2015).
[41] M. Ammon and J. Erdmenger, *Gauge/Gravity Duality: Foundations and Applications* (Cambridge University Press, Cambridge, England, 2015).
[42] H. Liu and J. Sonner, arXiv:1810.02367.
[43] A. Adams, P. M. Chesler, and H. Liu, Science **341**, 368 (2013).
[44] W. J. Li, Y. Tian, and H. B. Zhang, J. High Energy Phys. 07 (2013) 030.
[45] K. Murata, S. Kinoshita, and N. Tanahashi, J. High Energy Phys. 07 (2010) 050.
[46] M. J. Bhaseen, J. P. Gauntlett, B. D. Simons, J. Sonner, and T. Wiseman, Phys. Rev. Lett. **110**, 015301 (2013).
[47] M. Natsuume and T. Okamura, Phys. Rev. D **95**, 106009 (2017).
[48] S. R. Das and T. Morita, J. High Energy Phys. 01 (2015) 084.
[49] P. Basu and S. R. Das, J. High Energy Phys. 01 (2012) 103.
[50] P. Basu, D. Das, S. R. Das, and T. Nishioka, J. High Energy Phys. 03 (2013) 146.
[51] S. S. Gubser, Phys. Rev. D **78**, 065034 (2008).
[52] S. A. Hartnoll, C. P. Herzog, and G. T. Horowitz, Phys. Rev. Lett. **101**, 031601 (2008).
[53] C. P. Herzog, P. K. Kovtun, and D. T. Son, Phys. Rev. D **79**, 066002 (2009).
[54] See Supplemental Material at http://link.aps.org/supplemental/10.1103/PhysRevD.102.126005 for the equation of motion and the numerical scheme to simulate a temperature quench.
[55] K. Maeda, M. Natsuume, and T. Okamura, Phys. Rev. D **79**, 126004 (2009).
[56] K. Jensen, Phys. Rev. Lett. **107**, 231601 (2011).
[57] H. B. Zeng and H. Q. Zhang, Phys. Rev. D **98**, 106024 (2018).
[58] See Fig. 1 in the Supplemental Material for the distribution of $n^+$ and $n^-$ at three different sizes; $P(n^+)$ always equals $P(n^-)$.


*Correction:* The corresponding author byline footnote for the second author was missing at publication and has been inserted.